Ordering mechanism and spin fluctuations in a geometrically frustrated heavy-fermion antiferromagnet on the Kagome-like lattice CePdAl: A ^{27}Al NMR study

Akira Oyamada* and Satoru Maegawa
Graduate School of Human and Environmental Studies, Kyoto University, Kyoto 606-8501, Japan

Masahide Nishiyama
Department of Physics and Electronics, Osaka Prefecture University, Sakai, Osaka 599-8531, Japan

Hideaki Kitazawa
National Institute for Materials Science (NIMS), Tsukuba, Ibaraki 305-0047, Japan

Yosikazu Isikawa
Department of Physics, University of Toyama, Toyama 930-8555, Japan
(Received 1 May 2007; published 28 February 2008)

^{27}Al NMR measurements have been performed to investigate the ordering mechanism and spin fluctuations in a geometrically frustrated heavy-fermion antiferromagnet on the Kagome-like lattice CePdAl. This compound shows a partially ordered state below T_N (2.7 K), in which 1/3 of the Ce moments remain paramagnetic. Whether the remaining paramagnetic moments order at lower temperature or not has been controversial. Our NMR measurements show that the nuclear magnetic relaxation rate T_1^{-1} is proportional to the temperature below 0.2 K and there is no other phase transition down to 30 mK. The simulation of the spin echo spectra shows that the observed spectra are compatible with the partially ordered state and an incommensurate k vector along the c axis down to the lowest temperature. These results demonstrate that the paramagnetic Ce moments in the partially ordered state are in a heavy-fermion state and consequently the partially ordered state is considered to be stable down to 0 K. The temperature dependence of T_1^{-1} also shows that antiferromagnetic correlations develop from much higher temperatures above T_N.

DOI: 10.1103/PhysRevB.77.064432 PACS number(s): 76.50.+g, 71.27.+a, 75.10.Dg, 76.60.−k

I. INTRODUCTION

Geometrical frustration has attracted much attention recently because a rich variety of low temperature properties is expected due to the existence of many states energetically degenerated. Among the variety of low temperature properties, partially ordered states are one of the most interesting examples of the new type of magnetic orderings.

It has been proposed that the coexistence of geometrical frustration and instability of localized magnetic moments near the magnetic-nonmagnetic transition gives rise to a complicated magnetic phase diagram including the partially ordered state.[1,2] The instability of magnetic moments offers a new order parameter, the amplitute of the magnetic moments. One example is $R\mathrm{Mn}_2$ series of compounds (R=rare earth atom).[3] These compounds are nearly antiferromagnetic metals and exhibit instability of magnetic moments due to the itinerant character of the three-dimensional 3d electrons in the Mn atoms. DyMn_2 has been found to show a partially ordered state. Furthermore the temperature dependent amplitude of spin fluctuations of the Mn moments have been observed in YMn_2 by inelastic neutron scatterings.[4] Another example of the instability of magnetic moments is an f-electron system which shows the Kondo effect. In this case, the instability of the magnetic moments originates in the competition between the Kondo effect, which tends to cancel out the moments, and Ruderman-Kittel-Kasuya-Yosida (RKKY) interactions, which tend to form magnetic orderings. In order to examine this case, extensive studies of Ce and Yb compounds with geometrical frustration have recently been made. ZrNiAl-type compounds have a triangular arrangement of rare earth atoms and many attractive physical properties have also been reported, for example, valence fluctuation in CeRhSn,[5] multiple magnetic phase transitions in YbAgGe,[6] and a partially ordered state in CePdAl. In this paper we investigate the ordering mechanism and spin fluctuations of CePdAl by ^{27}Al NMR.

The crystal structure of CePdAl is of ZrNiAl type with space group $P\bar{6}2m$, as shown in Fig. 1.[7,8] Magnetic Ce ions form a network of regular triangles in the c plane, similar to the Kagome lattice. The number of nearest neighbors of each Ce atom is four in this compound, as well as in Kagome

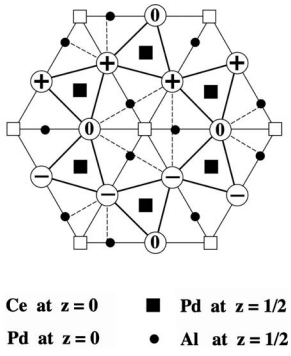

FIG. 1. Crystal structure and magnetic structure of CePdAl projected onto the c plane.

lattice compounds. However, the hexagons formed by the Ce atoms are distorted so that the number of next nearest neighbors is two, although the number is four in the case of the Kagome lattice. The distances between the nearest neighbor Ce atoms in c-axis and c-plane directions are 4.233 Å and 3.722 Å, respectively. The shorter distance in the c plane suggests the strong two-dimensional magnetic correlations.

The total spin J of Ce^{3+} is 5/2 ($L=3$, $S=1/2$). The degeneracy of the $J=5/2$ states lifts to three doublets in the crystal field. The ground state doublet can be viewed as effective spin 1/2 states. This compound shows typical properties of antiferromagnetic heavy-fermion compounds, namely antiferromagnetic ordering at 2.7 K ($=T_N$), the temperature dependence of the electrical resistivity $\rho \propto -\ln T$, and a large γ value (250 mJ/mol K^2) of the specific heat below T_N.[9–11] In addition, a large anisotropy of the magnetic susceptibility shows that the compound is an Ising-like system.

The most remarkable property of CePdAl is the partially ordered state. Neutron diffraction measurements of powder samples have shown that two thirds of the Ce moments order antiferromagnetically below 2.7 K (T_N) with a propagating vector $k=[1/2,0,0.35]$, while one third of the Ce moments remain paramagnetic, as shown in Fig. 1. Furthermore the magnetic structure is incommensurate along the c axis and remains a pure longitudinal sine wave down to 53 mK.[8] In order to explain the partially ordered state in CePdAl, a two-dimensional model of Ising spins with the Kondo effect and two kinds of exchange interactions on a Kagome-like lattice has been proposed by Dolores *et al.*[12] The model Hamiltonian (frustrated Kondo model) includes the nearest neighbor and the next nearest neighbor interactions between Ce atoms (J_1 and J_2, respectively) and the Kondo effect as follows:

$$H = \sum_i \Delta_i(T)|\mu_i^z|^2 - \frac{1}{2}\sum_{1\text{st.n.}} J_1 \vec{\mu_i^z}\cdot\vec{\mu_j^z} - \frac{1}{2}\sum_{2\text{nd.n.}} J_2 \vec{\mu_i^z}\cdot\vec{\mu_j^z}, \tag{1}$$

where Δ is the energy difference between a Ce Kondo state and a magnetic Ce state. A schematic view of the magnetic phase diagram is shown in Fig. 2. The paths of exchange interactions J_1 and J_2 are shown as solid and dotted lines, respectively. Model calculations showed that the observed magnetic structure appears in the region where $J_1>0$ and $J_2<0$ in the phase diagram, indicating that the magnetic structure is strongly affected by frustration of the antiferromagnetic interaction J_2. The model calculations also showed that the partially ordered state appears in the regions where $J_1<0$, $J_2>0$ and $J_1<0$, $J_2<0$.

Here we compare a Monte Carlo simulation for classical Ising spins on the Kagome lattice including J_1 and J_2, but not the Kondo effect.[13] The simulation showed that the partially ordered state is stable down to 0 K only in the region where $J_1<0$, $J_2<0$, indicated by the dark shaded area in Fig. 2. In other regions, ferromagnetic or ferrimagnetic states appear at lower temperatures. It is found that the Kondo effect and/or distortion of the Kagome lattice play important roles in extending the region where the partially ordered state is stable at 0 K to the upper and right-hand sides of the phase diagram

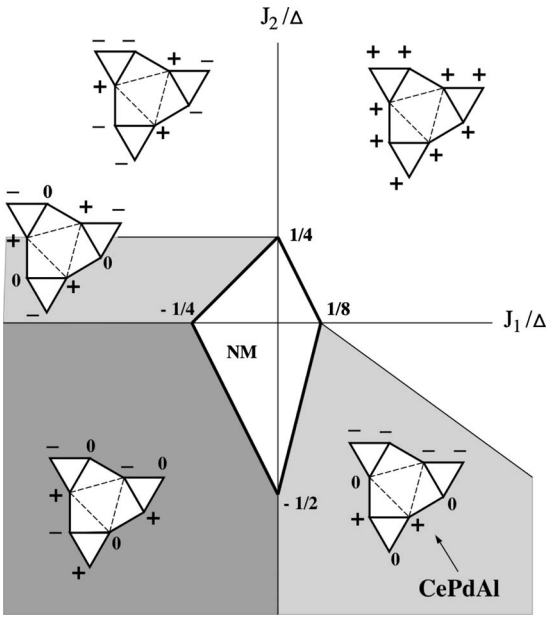

FIG. 2. Schematic view of the magnetic phase diagram reported by Dolores *et al.* using the Hamiltonian equation (1) (Ref. 12). The magnetic structures at 0 K are shown. NM indicates that there is no magnetic order. The dark shaded area ($J_1<0$, $J_2<0$) is the region where the partially ordered state is stable at 0 K in the classical Ising spin system on the Kagome lattice without the Kondo effect (Ref. 13). The light shaded areas are the extended regions where the partially ordered state is stable at 0 K due to the Kondo effect and/or distortion of the Kagome lattice.

(light shaded area in Fig. 2). The most interesting point is that CePdAl exists in this extended region. Therefore, it is crucial to determine whether 1/3 of the Ce moments remain paramagnetic down to 0 K to confirm the applicability of the model calculation.

However, the magnetic structure at 0 K is controversial. Dönni *et al.* reported that there is another phase transition below T_N, although the magnetic structure was not determined.[8] Furthermore, our previous NMR measurements showed that spin echo spectra consist of seven distinct peaks below T_N.[14] The spectra did not seem to be consistent with an incommensurate structure along the c axis at first glance. Recent precise neutron diffraction measurements have shown that there is no other phase transition below T_N and that the k vector is temperature dependent below T_N and constant below 1.9 K.[15]

Preliminary results of the spin echo spectra and relaxation rates between 1.5 K and 250 K have been reported in a previous paper.[14] In this paper we investigate the magnetic properties of CePdAl in more detail by ^{27}Al NMR measurements. We have measured spin echo spectra and spin-lattice relaxation rates down to 30 mK. We also discuss the magnetic structure at the lowest temperature and the antiferromagnetic correlations above T_N.

II. EXPERIMENTAL DETAILS

Details of the sample preparation of polycrystals and single crystals have been reported previously.[9,11] The

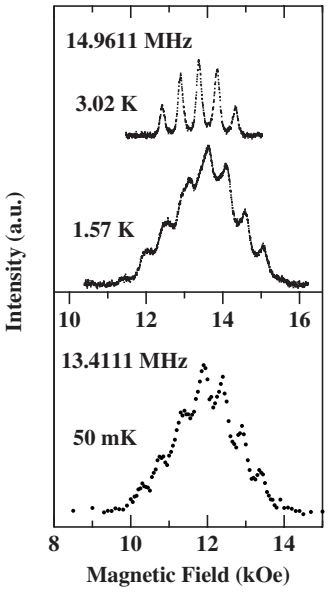

FIG. 3. NMR spectra of ^{27}Al nuclei at various temperatures. NMR frequencies are 14.9611 MHz at 3.02 K and 1.57 K, and 13.4111 MHz at 50 mK.

samples were ground to obtain powder samples to reduce the eddy currents in the NMR experiments.

^{27}Al ($I=5/2$) NMR measurements were performed with phase coherent spectrometers between 30 mK and 250 K. The operating frequencies were 14.9611 MHz between 1.5 K and 250 K and 13.4111 MHz between 30 mK and 1 K. Free powder samples were used for the NMR measurements, so that the samples orient such that the c axis (easy axis) is parallel to the applied magnetic field.

The rate T_1^{-1} is estimated from a fit of the recovery curve of the nuclear magnetization $M_z(t)$ for $I=5/2$ using the following equation:

$$\frac{M_z(\infty)-M_z(t)}{M_z(\infty)} = A\exp(-t/T_1) + B\exp(-6t/T_1) + C\exp(-15t/T_1). \quad (2)$$

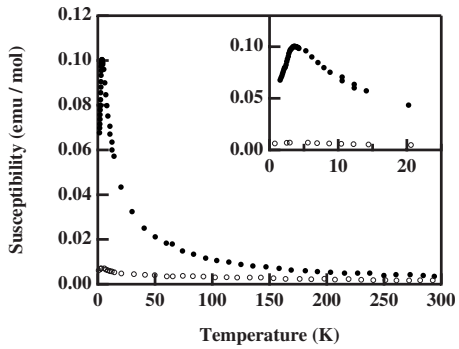

FIG. 4. Temperature dependence of susceptibilities. The filled and open circles show data for magnetic fields along the c axis and a axis, respectively. The inset shows the susceptibility around its maximum at low temperatures.

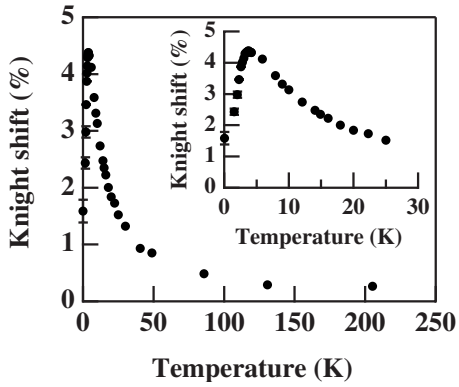

FIG. 5. Temperature dependence of Knight shift between 50 mK and 250 K. The inset shows the Knight shift around its maximum.

III. EXPERIMENTAL RESULTS

Spin echo spectra at various temperatures are shown in Fig. 3. The spectrum at 3.02 K above $T_N=2.7$ K consists of five peaks.

On the other hand, the spectrum below T_N consists of seven peaks. The structure of the spectra below T_N are the same down to 30 mK qualitatively.

The temperature dependence of the susceptibilities of CePdAl are shown in Fig. 4. The data for magnetic fields along the c axis and the a axis are shown as filled and open circles, respectively. The large anisotropy demonstrates that the system is Ising-like.

Figure 5 shows the temperature dependence of the Knight shift between 50 mK and 250 K. The Knight shift increases monotonously with decreasing temperature from 250 K down to 4 K. The shift has a broad maximum around 4 K and decreases below the temperature.

The Knight shift versus magnetic susceptibility plot (K-χ plot) in the temperature range between 250 K and 2 K is shown in Fig. 6, where the magnetic susceptibility of a single crystal under a magnetic field along the c axis is used.[11] The data above and below T_N are shown by filled and open circles, respectively. The figure indicates that the Knight shift is proportional to the susceptibility above T_N, which indi-

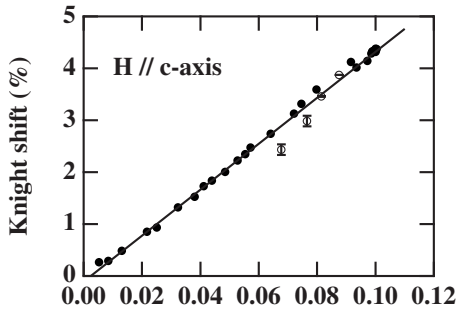

FIG. 6. Knight shift versus magnetic susceptibility. The filled and open circles show the data above and below T_N, respectively.

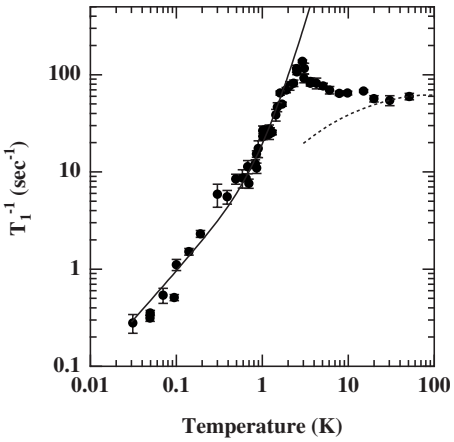

FIG. 7. Temperature dependence of the relaxation rate T_1^{-1} between 30 mK and 100 K. The solid line shows the fitting curve $T_1^{-1}=AT+BT^3$, where A and B are fitting parameters. The dotted line shows the χT curve.

cates that the hyperfine interaction between the ^{27}Al nuclei and the surrounding Ce moments is constant above T_N, even around the maximum of the Knight shift. The estimated hyperfine interaction (A_{hf}) is 2.47 kOe/μ_B. Below T_N, the plot starts to deviate slightly from the linear relation as the susceptibility becomes larger than the value expected for the linear relation. The deviation might be due to impurity effects.

Figure 7 shows the relaxation rate T_1^{-1} as a function of temperature. The peak at 2.7 K indicates the magnetic phase transition. The rate T_1^{-1} increases gradually with decreasing temperature above T_N, while T_1^{-1} decreases steeply below T_N. The dotted line shows the χT curve. Between T_N and 30 K, T_1^{-1} is not proportional to χT, suggesting the development of short range correlations.

The temperature dependence of T_1^{-1} below T_N is well described by the fitting curve $T_1^{-1}=AT+BT^3$, with $A=9.5$ s^{-1} K^{-1} and $B=11$ s^{-1} K^{-3}, as shown by the solid line in Fig. 7. Below 0.2 K, T_1^{-1} approaches a T-linear relation, which suggests the existence of continuous low-lying excited states.

IV. ANALYSIS AND DISCUSSION

A. Magnetic structure at 0 K

As mentioned in the Introduction, whether 1/3 of the Ce moments remain paramagnetic down to 0 K is the crucial issue. In this section, we first discuss whether the NMR spectra are compatible with the magnetic structure proposed by Keller *et al.* Second, we investigate the low temperature properties of the paramagnetic moments and discuss the magnetic structure at 0 K.

First we simulate the NMR spectra. The total Hamiltonian for a ^{27}Al nucleus is

$$\mathcal{H} = -\gamma_N \hbar H I_{z'} + \frac{e^2qQ}{4I(2I-1)}\{(3I_z^2 - I^2) + \eta(I_x^2 - I_y^2)\}, \quad (3)$$

where γ_N is the nuclear gyromagnetic ratio of ^{27}Al, I is the nuclear spin operator, eQ is the quadrupole moment of the nucleus, eq is the electric field gradient, and η is the asymmetry parameter. H is the sum of the applied magnetic field and the internal field; $H=H_0+H_{int}$. The suffix z means the principal axis of the electric field gradient, i.e., the c axis, and z' means the direction of the total field at Al sites. We note that the direction of the applied magnetic field does not correspond to the principal axis of the electric field gradient in general. The electric quadrupole frequency, $\nu_Q = 3e^2qQ/\{2I(2I-1)h\}$, and η have been estimated to be $\nu_Q = 0.542$ MHz and $\eta=0.27$ in our previous work.[14] We diagonalize the Hamiltonian to obtain eigenvalues and eigenvectors numerically. Using the obtained eigenvalues and eigenvectors, NMR spectra are obtained as the resonance energy between the energy levels for $\Delta I_z = \pm 1$. The spectrum in Fig. 8(a) shows the simulated and the experimental spectra at 3.02 K above T_N. The experimental spin echo spectra are shown as thick lines and the simulated spectra are shown as thin solid lines. The simulated spectra agree well with the observed spectra. The internal field H_{int} is zero, and the five peaks come from the quadrupole effects for $I=5/2$.

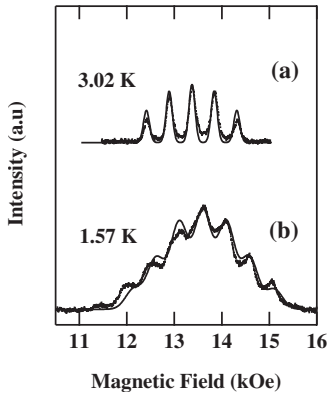

FIG. 8. NMR spectra at 3.02 K and 1.57 K. The thick lines are the experimental spin echo spectra and the thin solid lines are the simulated spectra.

Figure 8(b) shows the simulated and observed spectra at 1.57 K below T_N. In order to simulate the NMR spectra in the ordered state, we assume that the magnetic structure is partially ordered and the propagating vector is [1/2,0,0.35], as proposed based on neutron diffraction measurements.[15] The internal field H_{int} at ^{27}Al sites is considered to be originated from the surrounding ordered Ce moments through transferred hyperfine and dipolar interactions. We assume that the transferred hyperfine interactions (THI) are isotropic and we ignore the contribution from 1/3 of the paramagnetic moments, as will be discussed later. We take into account only the nearest neighbor 6 Ce moments for the THI. The dipolar field is estimated as the sum of the contributions from the Ce moments in $20\times20\times20$ unit cells. The shift of the resonant field and the magnitude of the THI are used as fitting parameters in the simulation. The distinct seven peaks in Fig. 8(b) are explained by the simulation as follows. The simulation demonstrates that there are three groups of Al sites in the partially ordered states, although there are many kinds of Al sites with slightly different internal fields in each group because of the incommensurate structure. The internal

field at the first group is positive, that of the second group is negative, and that of the third group is almost zero. As the magnitude of the internal field is roughly the same as the eqQ splitting, the spectrum consists of seven peaks. Furthermore, the peaks are widened because each group includes many kinds of sites. The simulation on the above assumptions fits well with the experimental spectrum in the ordered state. The important point of the spectra simulation is that there are three groups of Al sites in the partially ordered states, and the internal field of one of the three groups is almost zero. If we assume that the disordered moments in the partially ordered state order in any magnetic structures, there are no Al sites of which the internal field is almost zero. The observed spectra cannot be explained by the fully ordered spin structures. Therefore we conclude that the observed spin echo spectra indicate the partially ordered state.

We now comment on three points. First, we note that neutron diffraction measurements demonstrated that the z component of the k vector varies from 0.356 at 2.8 K to 0.351 at 0.18 K.[15] However, the spin echo spectra cannot distinguish such a small temperature dependence of the propagating vector because such a small variation of the k vector results in only a slight change of the intensity of the seven peaks. The next point is that the magnitude of THI is obtained to be 1 kOe/μ_B from the simulation and is smaller than the value of 2.8 kOe/μ_B obtained from the K-χ plot. A similar discrepancy has been reported for $CeAl_2$.[16] The width of the nuclear quadrupole resonance (NQR) spectra was 90 Oe, though the width expected from the THI is 3 kOe. One possible explanation for this discrepancy is the cancellation of the THI. If we simply assume that the mechanism of the THI is a RKKY interaction between a Ce moment and a ^{27}Al nuclear spin, the THI is an oscillating function of the distance between the Ce moment and the ^{27}Al nuclear spin. The contribution from the Ce moments which are far away from a ^{27}Al nucleus can induce the cancellation of the THI. The third point is the magnetic structure along the c axis. As mentioned before, it has been reported by the neutron experiments that the magnetic structure is incommensurate along the c axis and remains a pure longitudinal sine wave down to 53 mK.[8] In usual magnetic materials, a pure sine wave structure is stable only near T_N and a squaring up occurs at lower temperature. The stability of the sine wave structure down to lowest temperature implies that next three conditions are realized in CePdAl: (i) a competition between positive and negative long range interactions along the c axis due to the RKKY interactions, (ii) a large easy-axis-type anisotropy which favors sine wave structure to helical structure, and (iii) the Kondo effect that originates the moment reduction. We note that the Kondo effect is important even for the ordered moments. The similar sine wave structure has been reported in the heavy-fermion antiferromagnet $CeAl_2$.[17,18]

B. Spin fluctuations below T_N

The temperature dependence of T_1^{-1} below T_N is explained by the fitting curve $AT+BT^3$, as shown in Fig. 7. The term AT represents the contribution of the heavy-fermion state. The term BT^3 suggests the two magnon processes of the antiferromagnetic spin wave excitations.

The relaxation rate approaches T_1T=constant below 0.2 K. This result suggests that CePdAl is in the Fermi-liquid state at low temperatures. Therefore, 1/3 of the paramagnetic moments are in the heavy-fermion state and hence the localized moments of 1/3 of the Ce atoms disappear. Consequently, no other magnetic phase transition is expected below T_N and the magnetic structure in CePdAl is partially ordered even at 0 K. The specific heat divided by the temperature decreases with decreasing temperature below T_N and approaches the constant value 250 mJ/mol K^2.[10] This is consistent with our results. Both the frustrated exchange interactions and the formation of the heavy-fermion state are crucial for the magnetic structure in CePdAl. Our results support the theoretical explanation of Dolores *et al.*[12] Here we have to note that the magnetic structure is incommensurate along the c axis. As mentioned before, there is no squaring up of the magnetic structure and it remains a pure sine wave. Thus the Kondo effect is relevant not only for the disordered Ce moments but also for the other ordered Ce moments. Therefore the ordered moments also contribute to the observed T_1T=constant behavior.

C. Spin fluctuations above T_N

1. Antiferromagnetic fluctuations

In this section, we discuss the antiferromagnetic fluctuations above T_N. First, we discuss the maximum of the susceptibility around 4 K, shown in Fig. 4, from the microscopic point of view. We consider two possibilities: a heavy-fermion state and antiferromagnetic short-range correlations.

A similar maximum of the susceptibility has been observed in some compounds, such as $CeSn_3$, YbCuAl,[19] which show heavy-fermion behavior or valence fluctuations. At temperatures below the maximum, the K-χ plot of these materials deviates from a linear relation. In Ce and Yb compounds, the Knight shift becomes, respectively, larger and smaller than that expected from a linear relation. This deviation is well explained by theoretical calculations using the Anderson model.[20] The theory shows that the Kondo screening cloud surrounding a magnetic moment that develops at low temperatures gives rise to temperature dependence of the hyperfine interaction at nuclear sites. In contrast, the K-χ plot of CePdAl does not deviate from the linear relation, as shown in Fig. 6. Thus the maximum cannot be ascribed to the heavy-fermion state.

We now examine the second possibility, the antiferromagnetic short-range correlations. Figure 9 shows the temperature dependence of $(T_1T)^{-1}$ (filled circles) and the magnetic susceptibility with the magnetic field along the c axis (open circles). Both the magnetic susceptibility and Knight shift have maxima around 4 K, as shown in Fig. 5. This confirms that the uniform spin susceptibility, which is the $q=0$ component of χ, decreases below 4 K.

On the other hand, the value of $(T_1T)^{-1}$ increases with decreasing temperature below 50 K, and continues to increase around 4 K where the magnetic susceptibility and Knight shift show maxima. The value of $(T_1T)^{-1}$ is proportional to the q summation of the q-dependent spin susceptibility $\chi(q)$. The increase of $(T_1T)^{-1}$ means that the $q\neq 0$

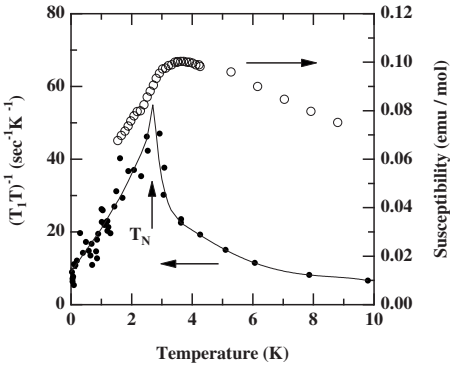

FIG. 9. Temperature dependence of $(T_1T)^{-1}$ (filled circles) between 30 mK and 10 K and the magnetic susceptibility along the c axis (open circles) between 1.5 K and 10 K. The solid curve is a guide for the eye.

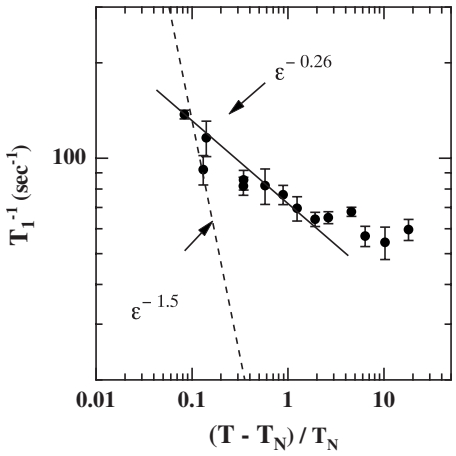

FIG. 10. T_1^{-1} vs ϵ plot.

component of $\chi(q)$ develops while the uniform spin susceptibility decreases below 4 K. This shows that antiferromagnetic short-range correlations are the origin of the broad maximum of the susceptibility.

2. Comparison with s=1/2 two-dimensional antiferromagnetic Ising model

The relaxation rate T_1^{-1} is generally given as follows:

$$T_1^{-1} = \frac{1}{2}\gamma_N^2 \int \langle h_+(0)h_-(t)\rangle e^{i\omega t}dt, \tag{4}$$

where $h_\pm$ are the fluctuating transverse hyperfine fields at Al sites. If we assume that the autocorrelation function of $4f$ electrons decays exponentially and that the susceptibility has no q dependence, T_1^{-1} is proportional to $\chi(0)T/\Gamma$, where Γ is the decay rate of the autocorrelation function. In magnetic materials with localized moments, T_1^{-1} is proportional to $\chi(0)T$ at high temperatures, as the Γ is independent of the temperature and $\chi(0)T$ is constant at high temperature.[19] However, as is shown in Fig. 7, T_1^{-1} below 30 K is not proportional to $\chi(0)T$ in CePdAl. In many heavy-fermion antiferromagnets, T_1^{-1} is almost constant above T_N and is not proportional to $\chi(0)T$, just the same as CePdAl. The origin of the constant T_1^{-1} is as follows. The susceptibility of the heavy-fermion antiferromagnets obey the Curie-Weiss law above the Kondo temperature so that T_1^{-1} is not proportional to $\chi(0)T$. On the other hand, Γ has temperature dependence originated by the Kondo effect. Then the counterbalance of the Curie-Weiss law to the temperature dependence of the Γ leads to the constant T_1^{-1}. This situation has been observed in typical heavy-fermion compounds.[21–23] Furthermore, the temperature dependence of Γ deduced by NMR measurements is consistent with that estimated by inelastic neutron experiments. Neutron experiments also show that Γ has no q dependence. In particular, $CePd_2Al_3$ is a good example which is quite similar to CePdAl with almost the same Kondo temperature and T_N. In the case of $CePd_2Al_3$, the Q component of the hyperfine interaction $(A(Q))$ is zero at Al sites, where Q is the ordering wave vector. Therefore Al-NMR measurements cannot observe the fluctuation mode of the Q vector. It has been reported that T_1^{-1} is actually constant above T_N in $CePd_2Al_3$.[24] Then we can assume that the Kondo fluctuation gives the constant T_1^{-1}, and the enhancement of T_1^{-1} below 10 K in CePdAl is ascribed to the development of the short-range correlations.

In order to discuss the short-range correlations, we use the Fourier transformation of the $4f$ spins,

$$S_q^z = N^{-1/2}\sum_i S_i^z \exp(i\mathbf{q}\cdot\mathbf{R}_i). \tag{5}$$

Then T_1^{-1} is given as follows:

$$T_1^{-1} = \frac{1}{2}\gamma_N^2 \int \langle h_+(0)h_-(t)\rangle e^{i\omega t}dt = \gamma_N^2 \frac{1}{N}A_{hf}^2 \sum_q \frac{|S_q^z|^2}{\Gamma_q}. \tag{6}$$

In order to discuss the critical behavior, we apply the static and dynamic scaling theory to analyze the relaxation rate above T_N. In this case, the equations $|S_q|^2=\xi^{2-\eta}f(q\xi)$, $\Gamma_q=\Gamma_c g(q\xi)$ and $\Gamma_c=\omega_{ex}\xi^{-z}$ can be assumed where ξ is the correlation length, and f and g are the homogeneous functions of the scaling law. Hence, T_1^{-1} is given as[25]

$$T_1^{-1} = (\gamma_N A_{hf})^2 \xi^{z-\eta}/\omega_{ex}. \tag{7}$$

For the two-dimensional antiferromagnetic Ising model (2DAFI model), $z=2-\eta$ and $\eta=0.25$, giving $z-\eta=1.5$. The correlation length ξ is proportional to ϵ^{-1}, where $\epsilon=(T-T_N)/T_N$.[26] Actually, the correlation length ξ is proportional to ϵ^{-1} in some 2DAFI systems, for example, Rb_2CoF_4,[27] UN,[28] and $Pb_2Sr_2TbCu_3O_8$.[29] Then, the temperature dependence of T_1^{-1} is given as

$$T_1^{-1} \propto \epsilon^{-1.5}. \tag{8}$$

The plot of T_1^{-1} vs ϵ in Fig. 10 indicates that T_1^{-1} is roughly proportional to $\epsilon^{-0.26}$ and is far from $\epsilon^{-1.5}$. Therefore the 2DAFI model cannot be applied to the spin fluctuations in CePdAl although the system is two-dimensional Ising-like. Here we note that the usual 2DAFI-type critical behavior may exist very close to T_N; however, the experimental accuracy of the relaxation rates is not enough for the nearer temperature region. Furthermore a 2D to 3D crossover may exist very close to T_N. In the case of the 3D antiferromag-

netic Ising model (3DAFI), T_1^{-1} is proportional to $\epsilon^{-1.92}$. This temperature dependence has not been observed in CePdAl.

The enhancement of T_1^{-1} in a rather wide temperature range was also reported in some frustrated antiferromagnets, for example, potassium jarosite $KFe_3(OOH)_6(SO_4)_2$ and $NiGa_2S_4$.[30,31] In those reports, the enhancement of T_1^{-1} is not explained by the usual critical behavior and is ascribed to the temperature dependence of the Γ,

$$\Gamma = \exp\left(-\frac{\Delta}{T}\right), \tag{9}$$

and it is also assumed that $\chi(q)$ has no temperature dependence. The problem is how ξ and/or Γ develop with decreasing temperature. We compare two models with our experimental results as follows.

3. Comparison with s=1/2 two-dimensional antiferromagnetic Heisenberg and the vortex model

At first, we compare our experimental results with the two-dimensional antiferromagnetic Heisenberg model (2DAFH model) because the temperature dependence of T_1^{-1} above T_N in CePdAl is similar to that in potasium jarosite ($S=5/2$)[30] and La_2CuO_4 ($S=1/2$), which are typical examples of a two-dimensional Heisenberg system. The $S=1/2$ 2DAFH model explains the temperature dependence of the correlation length in La_2CuO_4 well.[25] In this comparison, we assume that both ξ and Γ develop above T_N and are connected to each other by the dynamical scaling law. The critical coefficients are given as $z=d/2=1$ and $\eta=0.2$ for two-dimensional Heisenberg antiferromagnets, and these values give $z-\eta=0.8$. The correlation lengths of the 2DAFH model are given for classical spins and quantum spins as[32–34]

$$\xi/a = \exp[2\pi J_f S(S+1)/k_B T] \quad \text{(for classical spins)}, \tag{10}$$

$$\xi/a = C_\xi \exp(2\pi\rho_s/k_B T) \quad \text{(for quantum spins)}, \tag{11}$$

respectively, where C_ξ is a constant that is of the order of one, ρ_s is the spin-stiffness constant and if J_f is the exchange interaction. The relaxation rate is expressed for both cases as

$$T_1^{-1} \propto \exp(\delta/kT)^{0.8}/\omega_{ex}. \tag{12}$$

This model explains the experimental results quantitatively well, as shown in Fig. 11. The solid line in Fig. 11 shows the fitting curve $T_1^{-1}=50\times\exp(2.5/kT)^{0.8}$, $\delta=2.5$ K. It is not possible to determine whether the correlation length for classical spins [Eq. (8)] or that for quantum spins [Eq. (9)] is valid, because the exact value of the exchange interactions and the spin stiffness constant are unknown. The same fitting of T_1^{-1} for potassium jarosite gives $\delta=87$ K. These values are close to each T_N: 65 K for potassium jarosite and 2.7 K for CePdAl. The fact that these δ are remarkably close to T_N suggests that the spin fluctuations above T_N in CePdAl are well explained by the 2DAFH model.

In order to investigate the correlation length more quantitatively, we estimate the exchange frequency in CePdAl. The exchange frequency ω_{ex} is given as

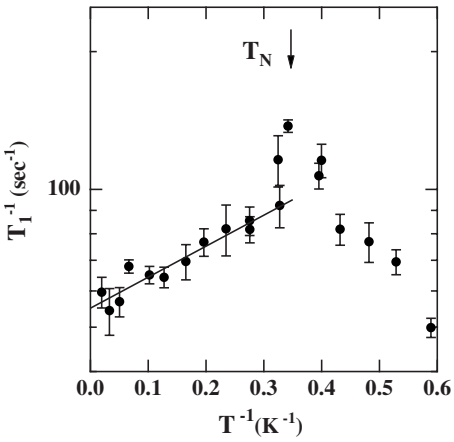

FIG. 11. T_1^{-1} vs T^{-1} plot between 1.6 K and 60 K. The solid line indicates $T_1^{-1}=50\times\exp(2.5/kT)^{0.8}$.

$$\omega_{ex} = \left\{\tfrac{8}{3} n_1 S_{eff}(S_{eff}+1)\right\}^{1/2} J_f/\hbar, \tag{13}$$

where $n_1=4$ is the number of nearest neighbor Ce atoms around a Ce atom, and S_{eff} is the effective spin.[35] Assuming $S_{eff}=1/2$, we estimate the exchange frequency as follows. In magnetic materials having localized moments, T_1^{-1} is constant in the paramagnetic phase at high temperatures, as follows:

$$T_1^{-1} = (2\pi)^{1/2}\gamma_N^2 g_{eff}^2 \left(\frac{A_{hf}^2}{n_2}\right)\frac{J(J+1)}{3}\frac{1}{\omega_{ex}}, \tag{14}$$

where n_2 is the number of the nearest neighbor Ce atoms around an Al atom. The constant value of T_1^{-1} in CePdAl at high temperatures is about 54 sec^{-1} and the experimental value of A_{hf} is 2.47 kOe/μ_B. From Eqs. (13) and (14), we estimate the exchange frequency $\omega_{ex}=5.7\times10^{12}$ Hz and the exchange interaction $J_f=31$ K. There is no accurate information on the exchange interaction in CePdAl. However, the value of J_f seems to be rather reasonable because it is close to the Weiss temperature of −30 K for a magnetic field parallel to the c axis. The exchange interaction in CePdAl must be much larger than T_N, as the frustration and Kondo effect lower the transition temperature. Using Eq. (7), the estimated ω_{ex} and A_{hf} give a correlation length of $\xi/a=2.3$ at 3 K. The correlation length in the frustrated system is rather small, even near the magnetic transition temperature. The small correlation length in CePdAl can be ascribed to the frustration.

As discussed above, the temperature dependence of the relaxation rate above T_N does not obey a power law, as shown in Fig. 7, but rather is proportional to $\exp(\delta/kT)^{0.8}$, as shown in Fig. 11. To the best of our knowledge, there have been no reports of the $\exp(\delta/kT)^{0.8}$ dependence of T_1^{-1} for Ce compounds. We note that similar behavior has been observed in potassium jarosite $KFe_3(OH)_6(SO_4)_2$, which is a good example of a two-dimensional Heisenberg antiferromagnet on a Kagome lattice.[30] This similarity between potassium jarosite and CePdAl suggests that the spin fluctuations above T_N in CePdAl can be explained by the two-dimensional Heisenberg model. We have already pointed out that the low-energy excitation does not have an energy gap

below T_N. This is also consistent with the Heisenberg model. The estimated correlation length may be too small to apply the scaling assumption, although the estimation of the absolute value should be regarded as an order estimation.

Second, we compare the vortex model with our experimental results. In this case, we assume that ξ and Γ are completely decoupled and only Γ develop above T_N. Figure 11 shows that T_1^{-1} is proportional to $\exp(\delta/kT)$ although the $\exp(\delta/kT)^{0.8}$ behavior previously discussed and $\exp(\delta/kT)$ behavior cannot be distinguished in this temperature range. Similar temperature dependence is reported in some frustrated magnets, $KFe_3(OH)_6(SO_4)_2$, $NiGa_2S_4$, $HCrO_2$, and $LiCrO_2$.[30,31,36] In the case of two dimensional Heisenberg systems $HCrO_2$ and $LiCrO_2$, Ajiro *et al.* proposed that the electron paramagnetic resonance (EPR) linewidth is inversely proportional to the thermally excited vortex density which is proportional to $\exp(-E_v/kT)$, with E_v the activation energy of the vortices. The thermally excited Z_2 vortices had been suggested theoretically in 2D Heisenberg triangular antiferromagnets and those vortices undergo a Kosterlitz-Thouless-like transition at T_{KM} with $E_v=5kT_{KM}$.[37] Even in Ising triangular antiferromagnets, each triangle has six equivalent magnetic states and the six-clock states are able to make vortex excitations that lead to a Kosterlitz-Thouless-like transition.[38,39] Thus the vortex excitations may dominate the temperature dependence of T_1^{-1} above T_N in CePdAl although CePdAl is an Ising-like Kagome antiferromagnet. In this context, the vortices might be excited at high temperatures in CePdAl, however, the interactions between the triangular lattice planes lead to three-dimensional ordering at T_N, which is higher than T_{KM}.

We discussed the two models at the two limits. First, the 2DAFH model which assumes the dynamical scaling between ξ and Γ was discussed, and second the vortex model which assumes only the temperature dependence of Γ were also discussed. However, we cannot conclude which model described the physical properties of CePdAl best. The most important point is that the relaxation rate T_1^{-1} above T_N shows critical behavior in a rather wide temperature range and is proportional to $\exp(\delta/kT)$. This seems to be a common characteristic of two-dimensional frustrated antiferromagnets. It is strongly required to study theoretically and experimentally how ξ and/or Γ develop with decreasing temperature.

V. CONCLUSION

^{27}Al NMR experiments were performed on CePdAl, a geometrically frustrated heavy-fermion compound on a Kagome lattice, to study the magnetic structure and spin fluctuations of this compound. The obtained NMR spectra below T_N confirm that the CePdAl has a partially ordered magnetic structure, as proposed based on neutron diffraction measurements. Furthermore, T_1T=constant law at low temperatures shows that the remaining paramagnetic moments are in a heavy-fermion state. These results suggest that cancellation of the magnetic moments by the Kondo effect relieves the frustration of the Kagome-like lattice and that the partially ordered state is stable down to 0 K. This is a new way of the relief of frustration due to instability of $4f$ electrons.

The temperature dependence of T_1^{-1} demonstrates that the antiferromagnetic spin correlations develop from the temperature far above T_N. This behavior seems to be a common characteristic of two-dimensional frustrated antiferromagnets. The experimental temperature dependence of T_1^{-1} is compared with the two-dimensional antiferromagnetic Heisenberg model and the vortex model. It is strongly required to study how ξ and/or Γ develop with decreasing temperature in frustrated antiferromagnets theoretically and experimentally.

ACKNOWLEDGMENTS

The authors wish to thank K. Kamioka and K. Hashi for their work in the initial stages of this study. The authors also thank T. Goto for valuable discussions. The numerical calculations were performed at the Academic Center for Computing and Media Studies, Kyoto University. This work was supported by Grant-in-Aid for Scientific Research on Priority Areas "Novel States of Matter Induced by Frustration" (Grant No. 19052005).

*f52017@sakura.kudpc.kyoto-u.ac.jp

[1] M. D. NunezRegueiro, C. Lacroix, and R. Ballou, Phys. Rev. B **46**, 990 (1992).
[2] R. Ballou, J. Alloys Compd. **275-277**, 510 (1998).
[3] R. Ballou, C. Lacroix, and M. D. NunezRegueiro, Phys. Rev. Lett. **66**, 1910 (1991).
[4] M. Shiga, H. Wada, Y. Nakamura, J. Deportes, B. Ouladdiaf, and K. R. A. Ziebeck, J. Phys. Soc. Jpn. **57**, 3141 (1988).
[5] M. S. Kim *et al.*, Phys. Rev. B **68**, 054416 (2003).
[6] K. Umeo, K. Yamane, Y. Muro, K. Katoh, Y. Niide, A. Ochiai, T. Morie, T. Sakakibara, and T. Takabatake, J. Phys. Soc. Jpn. **73**, 537 (2004).
[7] B. Xue, H. Schwer, and F. Hulliger, Acta Crystallogr., Sect. C: Cryst. Struct. Commun. **50**, 338 (1994).
[8] A. Dönni, G. Ehlers, H. Maletta, P. Fischer, H. Kitazawa, and M. Zolliker, J. Phys.: Condens. Matter **8**, 11213 (1996).
[9] H. Kitazawa, A. Matsushita, T. Matsumoto, and T. Suzuki, Physica B **199-200**, 28 (1994).
[10] C. Schank, F. Jährling, L. Luo, A. Grauel, C. Wassilew, R. Borth, G. Olesch, C. Bredl, C. Geibel, and F. Steglich, J. Alloys Compd. **207-208**, 329 (1994).
[11] Y. Isikawa, T. Mizushima, N. Fukushima, T. Kuwai, J. Sakurai, and H. Kitazawa, J. Phys. Soc. Jpn. **65**, 117 (1996).
[12] M. Dolores, Núñez-Regueiro, C. Lacroix, and B. Canals, Physica C **282-287**, 1885 (1997).
[13] T. Takagi and M. Mekata, J. Phys. Soc. Jpn. **62**, 3943 (1993).
[14] A. Oyamada, K. Kamioka, K. Hashi, S. Maegawa, T. Goto, and H. Kitazawa, J. Phys. Soc. Jpn. Suppl. B **65**, 123 (1996).

[15] L. Keller, A. Dönni, H. Kitazawa, and B. van den Brandt, Appl. Phys. A: Mater. Sci. Process. **74**, S686 (2002).
[16] D. E. MacLaughlin, O. Penna, and M. Lysak, Phys. Rev. B **23**, 1039 (1981).
[17] B. Barbara, J. X. Boucherle, J. L. Buevoz, M. F. Rossignol, and J. Schweizer, Solid State Commun. **24**, 481 (1977).
[18] S. M. Shapiro, E. Gurewitz, R. D. Parks, and L. C. Kupferberg, Phys. Rev. Lett. **43**, 1748 (1979).
[19] D. E. MacLaughlin, *Valence Fluctuations in Solids* (Elsevier, North-Holland, Amsterdam, 1981), p. 321.
[20] E. Kim and D. L. Cox, Phys. Rev. B **58**, 3313 (1998).
[21] T. Shimizu, M. Takigawa, H. Yasuoka, Y. Onuki, and T. Komatsubara, J. Phys. Soc. Jpn. **54**, 470 (1985).
[22] L. P. Regnault, W. A. C. Erkelens, J. Rossat-Mignod, P. Lejay, and J. Flouquet, Phys. Rev. B **38**, 4481 (1988).
[23] Y. Kitaoka, H. Arimoto, Y. Kohori, and K. Asayama, J. Phys. Soc. Jpn. **54**, 3236 (1988).
[24] H. Tou, Y. Kitaoka, K. Asayama, S. A. M. Mentink, G. J. Nieuwenhuys, A. A. Menovsky, and J. A. Mydosh, J. Phys. Soc. Jpn. **63**, 4176 (1994).
[25] J. H. Cho, F. Borsa, D. C. Johnston, and D. R. Torgeson, Phys. Rev. B **46**, 3179 (1992).
[26] M. F. Collins, *Magnetic Critical Scattering* (Oxford University Press, New York, 1989).
[27] E. J. Samuelsen, Phys. Rev. Lett. **31**, 936 (1973).
[28] T. M. Holden, W. J. L. Buyers, E. C. Svensson, and G. H. Lander, Phys. Rev. B **26**, 6227 (1982).
[29] S. Y. Wu, W. H. Li, K. C. Lee, J. W. Lynn, T. H. Meen, and H. D. Yang, Phys. Rev. B **54**, 10019 (1996).
[30] M. Nishiyama, S. Maegawa, T. Inami, and Y. Oka, Phys. Rev. B **67**, 224435 (2003).
[31] K. Ishida (private communication).
[32] A. M. Polyakov, Phys. Lett. **59**, 79 (1975).
[33] D. R. Nelson and R. A. Pelcovits, Phys. Rev. B **16**, 2191 (1977).
[34] S. Chakravarty, B. I. Halperin, and D. R. Nelson, Phys. Rev. B **39**, 2344 (1989).
[35] T. Moriya, Prog. Theor. Phys. **16**, 33 (1956).
[36] Y. Ajiro, H. Kikuchi, S. Sugiyama, T. Nakashima, S. Shamoto, N. Nakayama, M. Kiyama, N. Yamamoto, and Y. Oka, J. Phys. Soc. Jpn. **57**, 2268 (1988).
[37] H. Kawamura and S. Miyashita, J. Phys. Soc. Jpn. **53**, 4138 (1984).
[38] S. Miyashita, H. Kitatani, and Y. Kanada, J. Phys. Soc. Jpn. **60**, 1523 (1991).
[39] H. Otsuka, Y. Okabe, and K. Nomura, Phys. Rev. E **74**, 011104 (2006).